

## Supporting Information

### **Reversible Networked Porous Formation in Sb Nanoparticles during Cycles: Sb Nanoparticles Encapsulated into Nitrogen-Doped Carbon Matrix with Nanorods Structure for High-Performance Li-ion Batteries**

Ping Feng,<sup>a</sup> Zhe Cui,<sup>a</sup> Shu-Ang He,<sup>a</sup> Qian Liu,<sup>b</sup> Jingqi Zhu,<sup>a</sup> Chaoting Xu,<sup>a</sup> Rujia Zou<sup>\*a</sup> and Junqing Hu<sup>a,c</sup>

<sup>a</sup> State Key Laboratory for Modification of Chemical Fibers and Polymer Materials,  
College of Materials Science and Engineering, Donghua University, Shanghai 201620,  
China. E-mail: rjzou@dhu.edu.cn

<sup>b</sup> College of Science, Donghua University, Shanghai 201620, China

<sup>c</sup> College of Health Science and Environmental Engineering, Shenzhen Technology  
University, Shenzhen 518118, China

## **I. Experimental section**

### **1.1 Synthesis of SbPO<sub>4</sub> nanorods**

SbPO<sub>4</sub> nanorods as the sacrificial template were initially synthesized through a hydrothermal reaction. Typically, 0.228 g of SbCl<sub>3</sub>, 0.345g of NH<sub>4</sub>H<sub>2</sub>PO<sub>4</sub> were dissolved into 40 ml of ethylene glycol at room temperature. This dispersion was heated to 70 °C and transferred to a Teflon-lined stainless autoclave at 160 °C for 4 h in an electric oven. After being cooled to room temperature naturally, the precipitate was collected and washed with deionized water and ethanol several times by centrifugation, then dried at 60 °C overnight to obtain SbPO<sub>4</sub> nanorods.

## **1.2 Synthesis of hollow Sb<sub>2</sub>O<sub>5</sub> nanorods**

To prepare Sb<sub>2</sub>O<sub>5</sub> nanorods, 100 mg of the prepared SbPO<sub>4</sub> nanorods and 165mg KMnO<sub>4</sub> were added to 30 ml of deionized water under ultrasonication for 20 min. After the suspension was placed into a 100 ml flask and maintained at 75 °C for 12 h. After being cooled to room temperature naturally, the precipitate was collected and washed with deionized water and ethanol several times by centrifugation, then dried at 60 °C overnight to obtain hollow Sb<sub>2</sub>O<sub>5</sub> nanorods.

## **1.3 Synthesis of Sb@N-MC nanorod**

In a typical synthesis, 50 mg of Sb<sub>2</sub>O<sub>5</sub> powder was dispersed in 50 ml Tris-buffer solution (10 mM, pH =8.5) and sonicated for 30 min. To coat a polydopamine shell, 50 mg of dopamine hydrochloride was added in the solution and stirred for 2 h. The resultant brownish black solution was washed with DI water and ethanol for several times and then dried under vacuum overnight. The obtained dark brown powder was put into a tube furnace and annealed at 500 °C under Ar/H<sub>2</sub> atmosphere for 4 h with a heating rate of 2 °C min. After being cooled to room temperature naturally, Sb@N-MC nanorod was obtained.

## **1.4 Synthesis Sb nanoparticles**

Sb nanoparticles were synthesized by a wet chemical method. 0.45 g of NaBH<sub>4</sub> was dissolved in 13 mL of NMP in a three-necked flask under argon protection and heated to 60 °C. Subsequently, 0.68 g of SbCl<sub>3</sub> dissolved in 2 mL of NMP was immediately injected

via a syringe. The reaction mixture swiftly turned black and was cooled down quickly using an ice water bath. After cooling down to room temperature, the resultant Sb nanoparticles were collected by centrifugation, washed with deionized water several times, and dried at 40 °C overnight.

### **1.5 Synthesis SbNP@C nanoparticles**

Synthesis of Sb@C nanoparticles. 0.1g Sb nanoparticles were dispersed in 75ml ethanol/water solution (v/v 1:2), and then 0.25g 3-aminophenol, 0.075g hexadecyl trimethyl ammonium Bromide, 0.25ml formaldehyde solution, were added to start the reaction with 0.1ml ammonia aqueous solution as catalyst. The reacting solution was stirred continuously at room temperature for 30 min. And then, the resultant Sb@RF nanoparticles were collected by centrifugation, washed with deionized water several times, and dried at 40 °C overnight. Finally, the obtained Sb@RF powder was put into a tube furnace and annealed at 500 °C under Ar/H<sub>2</sub> atmosphere for 4 h with a heating rate of 2 °C min. After being cooled to room temperature naturally, SbNP@C nanoparticles was obtained.

## II. The thermogravimetric analysis of carbon content for Sb@N-CM nanorods

In order to ascertain carbon content for Sb-C composite materials, the thermogravimetric analysis (TGA) measurement has been conducted in air. As can be seen from Fig. 6, the slight weight loss for SbNP, Sb@N-CM nanorods, and SbNP@C is attributed to the adsorption of water below 300 °C. The weight gain of SbNP between 300~500 °C is due to the slightly oxidation of Sb to Sb<sub>2</sub>O<sub>3</sub> ( $4\text{Sb} + 3\text{O}_2 = 2\text{Sb}_2\text{O}_3$ ). However, the huge weight loss for Sb@N-CM nanorods, and SbNP@C is mainly attributed to the combustion of carbon to CO<sub>2</sub> and oxidation of Sb into Sb<sub>2</sub>O<sub>3</sub>. And then, the weight remains no change until 500 °C, indicating the entirely oxidation of the combustion of carbon to CO<sub>2</sub> and oxidation of Sb into Sb<sub>2</sub>O<sub>3</sub> for different samples. Finally, the carbon content of Sb@N-CM nanorods, and SbNP@C sample is calculated to ~33 and ~59%, respectively.

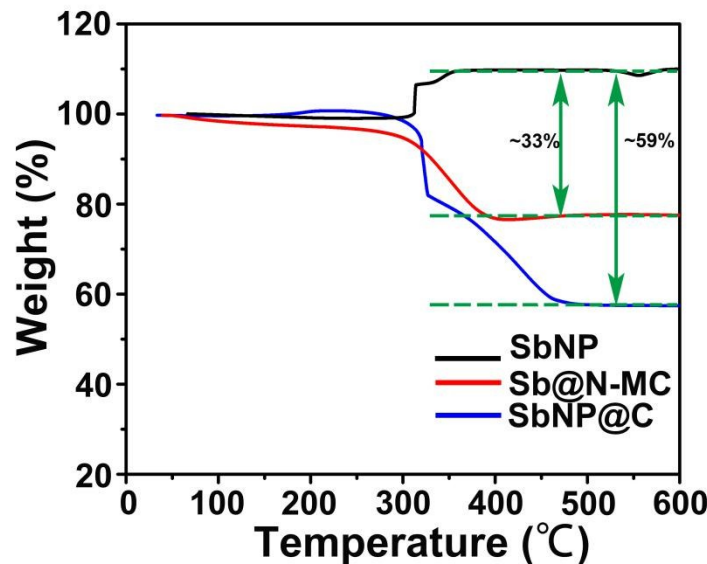


**Fig. S1.** TGA curves of SbNP, Sb@N-CM nanorods, and SbNP@C, respectively.

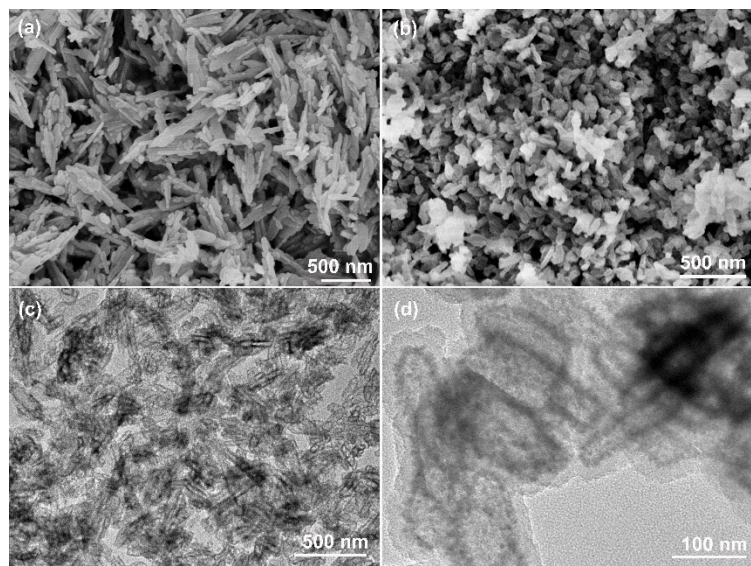


**Fig. S2** (a) SEM image of  $\text{SbPO}_4$  nanorods. (b, c) SEM and TEM image of porous  $\text{Sb}_2\text{O}_5$  hollow nanorods. (d) TEM image of hollow  $\text{PDA}@\text{Sb}_2\text{O}_5@\text{PDA}$  nanorods.

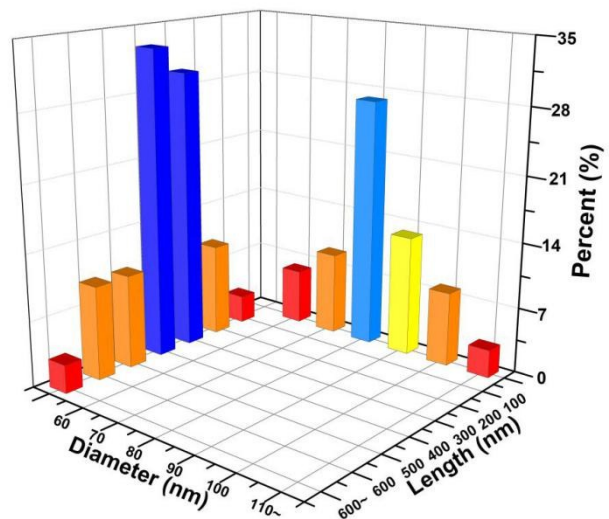


**Fig. S3.** The average diameter and length distribution of the  $\text{Sb}@\text{N-CM}$  nanorods.

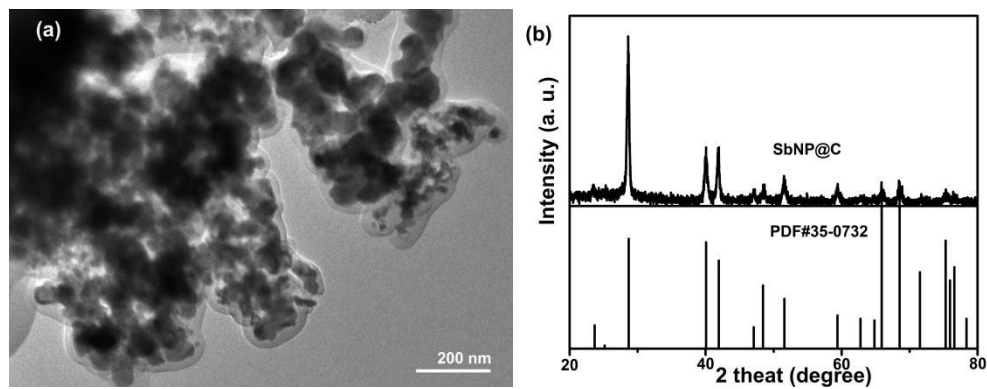


**Fig. S4** (a) TEM image of the Sb@C nanoparticles. (b) XRD pattern of the Sb@C nanoparticles.

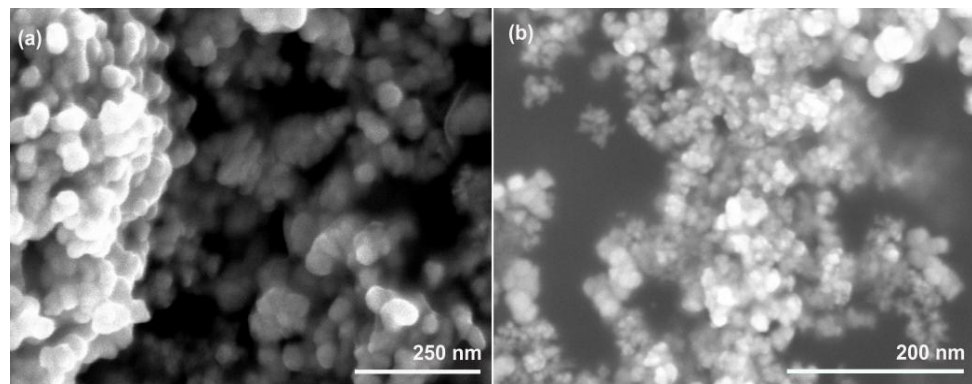


**Fig. S5** (a, b) SEM images of the Sb nanoparticles.

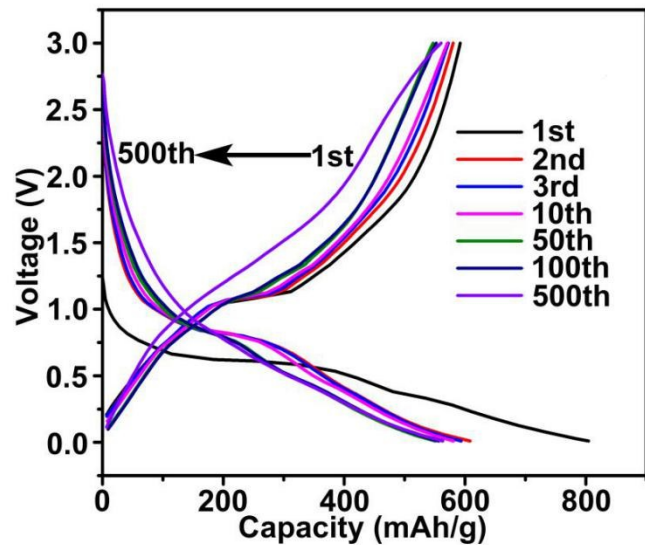


**Fig. S6.** The galvanostatic charge and discharge profiles of Sb@N-CM nanorods at a current density of 1000 mA g<sup>-1</sup> for different cycles.

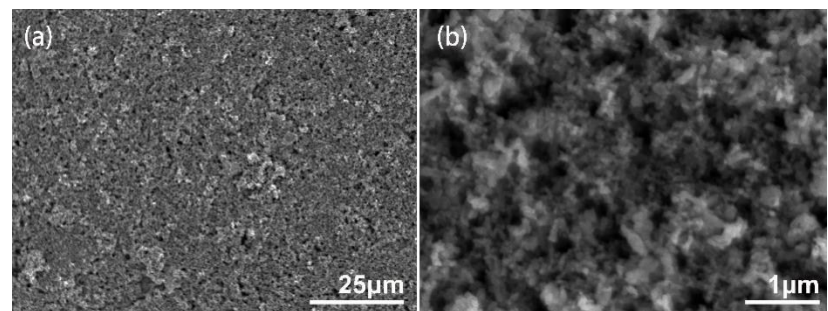


**Fig. 7** (a, b) the SEM images of the Sb@N-CM nanorods electrode before cycle.

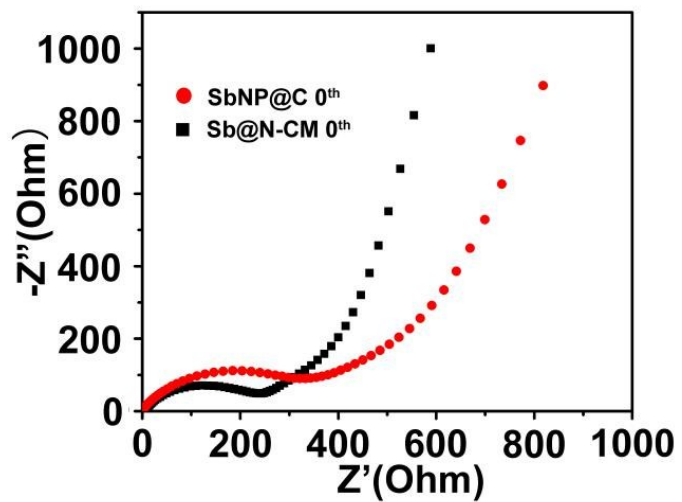


**Fig. S8.** The electrochemical impedance spectra of Sb@N-CM nanorods electrode and Sb@C nanoparticles electrode before cycles.

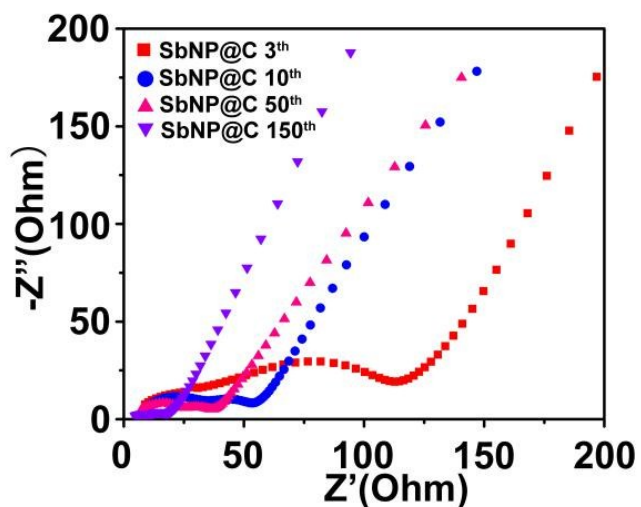


**Fig. S9.** The electrochemical impedance spectra of Sb@C nanoparticles electrode after different cycles.

**Table S1.** Comparison of the cycle performances of Sb@N-MC nanorod electrode with other Sb-based anode materials reported in the literature.

Electrodes	Current density (mA g <sup>-1</sup> )	Cycle number	Reversible capacity (mA h g <sup>-1</sup> )	Reversible capacity (mA h g <sup>-1</sup> )	capacity retention (%)	Ref.
Sb@N-MC nanorod	200	190	706.8	695.6	100.3	This work
	1000	500	593.5	591.8	99.7	
hollow Sb@C yolk-shell spheres	50 1000	100 300	680	525 405	77.2	13
Sb@TiO <sub>2-x</sub> nanotubes	660 3300 6600	1000 1000 1000		547 445 424		20
Sb@N-C	200 2000	300 3000	650.8 467.6	602.8 395	92.7 84.5	21
monodisperse Sb nanocrystals	330 2640	100 100	600			15
antimony/amorphous carbon/graphene	500 1000	400 700	665.4	592 413	88.9	19
SiO <sub>2</sub> /Sb@CNF	500 1000	400 400		572 468		14
C/Sb composites	100	200	595.5	466.2	78.3	25
G@NiSb/Sb@NF	200	50		340		18
ball milled Sb-carbon	230	250	612	550	89.8	29

Sb/NPC	200	100		556		30
rod-like Sb-C	100	100	687.1	478.8	69.7	31
Sb/graphene	100	40		411		32
	400	40		250		
RGO-SbTF-Ni	100	50	576.1	424.1	73.6	33
Sb/C composite	200	100	617	565	91.5	34
	1000	500		400.5		
Sb/carbon fiber	100	100	680	315.9	46.5	35

## References

13 J. Liu, L. Yu, C. Wu, Y. Wen, K. Yin, F. K. Chiang, R. Hu, J. Liu, L. Sun, L. Gu, J. Maier, Y. Yu and M. Zhu, *Nano Lett.*, 2017, **17**, 2034-2042.

20 N. N. Wang, Z. C. Bai, Y. T. Qian and J. Yang, *Adv. Mater.*, 2016, **28**, 4126-4133.

21 W. Luo, F. Li, J. J. Gaumet, P. Magri, S. Diliberto, L. Zhou and L. Q. Mai, *Adv. Energy Mater.*, 2018, **8**, 1703237.

15 M. He, K. Kravchyk, M. Walter and M. V. Kovalenko, *Nano Lett.*, 2014, **14**, 1255-1262.

19 Z. Z. Wang, J. Qu, S. M. Hao, Y. J. Zhang, F. Q. Kong and Z. Z. Yu, *ChemElectroChem*, 2018, **5**, 2653-2659.

14 H. K. Wang, X. M. Yang, Q. Z. Wu, Q. B. Zhang, H. X. Chen, H. M. Jing, J. K. Wang, S. B. Mi, A. L. Rogach and C. M. Niu, *ACS Nano*, 2018, **12**, 3406-3416.

25 Y. Cheng, Z. Yi, C. L. Wang, L. D. Wang, Y. M. Wu and L. M. Wang, *Chem. Asian J.*, 2016, **11**, 2173-2180.

18 Y. L. Ding, C. Wu, P. Kopold, P. A. van Aken, J. Maier and Y. Yu, *Small*, 2015, **11**, 6026-6035.

29 T. Ramireddy, M. M. Rahman, T. Xing, Y. Chen and A. M. Glushenkov, *J. Mater. Chem. A*, 2014, **2**, 4282-4291.

30 Q. Yang, J. Zhou, G. Zhang, C. Guo, M. Li, Y. Zhu and Y. Qian, *J. Mater. Chem. A*, 2017, **5**, 12144-12148.

31 L. Fan, J. J. Zhang, J. H. Cui, Y. C. Zhu, J. W. Liang, L. L. Wan and Y. T. Qian, *J. Mater. Chem. A*, 2015, **3**, 3276-3280.

32 Y. D. Zhang, J. Xie, T. J. Zhu, G. S. Cao, X. B. Zhao and S. C. Zhang, *J. Power Sources*, 2014, **247**, 204-212.

33 Z. Yi, Q. G. Han, Y. Cheng, F. X. Wang, Y. M. Wu and L. M. Wang, *Electrochim. Acta*, 2016, **190**, 804-810.

34 Z. Yi, Q. Han, P. Zan, Y. Wu, Y. Cheng and L. Wang, *J. Power Sources*, 2016, **331**, 16-21.

35 H. Lv, S. Qiu, G. Lu, Y. Fu, X. Li, C. Hu and J. Liu, *Electrochim. Acta*, 2015, **151**, 214-221.